Doctoral Forum on Vacuum Electronics (FVE 2017)

22–23 August 2017

0.85 THz truncated sine waveguide traveling-wave tube with sheet beam tunnel

Shuanzhu Fang[1], Jin Xu[1], Xuebin Jang[1], Xia Lei[1], Chong Ding[1], Qian Li[1], Gangxiong Wu[1], Ruichao Yang[1], Luqi Zhang[1], Minzhi Huang[1], Tao Tang[1], Guoqing Zhao[1], Zhanliang Wang[1], Wenxiang Wang[1], Jinjun Feng[2], Yubin Gong[1], Yanyu Wei[1]

[1]*National key Laboratory of Science and Technology on Vacuum Electronics, School of Physical Electronics, University of Electronic Science and Technology of China, No. 4, Section 2, North Jianshe Road, 610054 Chengdu, People's Republic of China*

[2]*Beijing Vacuum Electronics Research Institute, Beijing 100015, People's Republic of China*

E-mail: yywei@uestc.edu.cn

Published in *The Journal of Engineering*; Received on 7th February 2018; Revised on 19th April 2018; Accepted on 24th April 2018

Abstract: A sine waveguide (SWG) traveling-wave tube with sheet electron beam tunnel is proposed to amplify the high-frequency terahertz wave. In this study, the slow wave characteristics including the dispersion properties and interaction impedances have been investigated by using the eigenmode solver in the 3D electromagnetic simulation software Ansoft HFSS. The truncated SWG slow wave structure possesses the relatively large average coupling impedance. The beam–wave interaction characteristics of truncated SWG with sheet electron beam tunnel are calculated by high-frequency simulation software CST. From the particle-in-cell simulation results, this beam–wave interaction circuit can produce >490 mW ranging from 0.845 to 0.855 THz with a corresponding gain over 22 dB.

1 Introduction

Recently, terahertz science and technology has aroused wide public concern due to its great potential in the scientific and technological community [1–3]. The traveling-wave tube (TWT) is one of the most important vacuum electron devices for energy amplification in the terahertz band. Owing to their wide operation bandwidth, large output power and compact structure, the TWTs are very significant as the applicable terahertz radiation source [4, 5].

As the core component of TWT, the Slow-wave structure (SWSs) determine the performances of the device to a large extent. Nowadays, staggered double vane structure [6, 7], sine waveguide (SWG) [8–10], folded waveguide [11, 12], and double corrugation rectangular waveguide [13, 14] are suggested as the SWSs for TWTs operating in the millimetre wave and terahertz band.

In the sub-millimetre and terahertz bands, metal loss severely limits the output power of the entire TWT. Compared to other SWSs, SWG which possesses low ohmic losses and reflection is a promising slow wave structure for sheet electron beam terahertz TWT [15, 16]. This paper will present the high-frequency characteristics of truncated sine waveguide (TSWG) SWS, transmission characteristics of pillbox window and entire high-frequency system, and beam–wave interaction simulation results of the TSWG TWT with sheet electron beam tunnel.

2 Slow-wave structure characteristics

Fig. 1 shows the perspective view of the TSWG SWS model and single period structure, where a is the width of the waveguide, b is the height of the waveguide, h is the oscillating amplitude, p is the oscillating period, h_b is the height of the sheet beam tunnel. As shown in Fig. 1, the TSWG SWS evolves from the conventional SWG SWS by compressing the height of the waveguide and truncating the peak of the sine-shape metal gratings. In Fig. 1*b*, h_c represents the height of the part which is truncated [17].

The slow wave characteristic including dispersion properties and interaction impedance can be analysed by 3D electromagnetic simulation software Ansoft HFSS [18]. In our analysis, it is assumed that the voltage of the electron beam is 18.85 kV and the height of the sheet beam tunnel is 30 μm. After the optimisation process, the optimised structure parameters are obtained as follows: $a = 195$, $b = 125$, $p = 112.5$, $h = 52.5$, $h_b = 30$, $h_c = 5$ μm. As shown in Fig. 2*b*. When $h_c = 5$ μm, the interaction impedances in the frequency range of 0.8–1 THz are maximum. The tradeoff between the dispersion relation and interaction impedance should be made in our design. To achieve the maximum interaction impedance, the value of the height h_c is selected to be 5 μm. Fig. 2 shows the simulation results of the dispersion relation and interaction impedance of the TSWG SWS. From the calculated results shown in Fig. 2, we can see that the TSWG SWS has a wide cold bandwidth 0.75–1 THz.

3 Transmission characteristics of high-frequency system

The transmission model is comprised of 150 main periods and six periods of transition couplers. The *S*-parameters of the model have been calculated by using the transient solver in the CST MWS [19]. The material of the transmission model is set as oxygen-free high-conductivity copper with conductivity of 1.2×10^7 S/m [20], considering the non-ideal surface roughness of the metal walls. From Fig. 3, it can be seen that the reflection parameter S_{11} of the TSWG circuit model is less than −30 dB within the operating frequency range from 0.8 to 1 THz. The transmission parameter S_{21} of the TSWG circuit model is more than −15 dB in the frequency range from 0.8 to 1 THz. For 0.85 THz, the TSWG circuit has a loss of 0.813 dB/mm.

4 Input/output structure

The output RF vacuum window is a critical component of vacuum electronic devices. It is generally used to separate the high vacuum

doi: 10.1049/joe.2018.0099

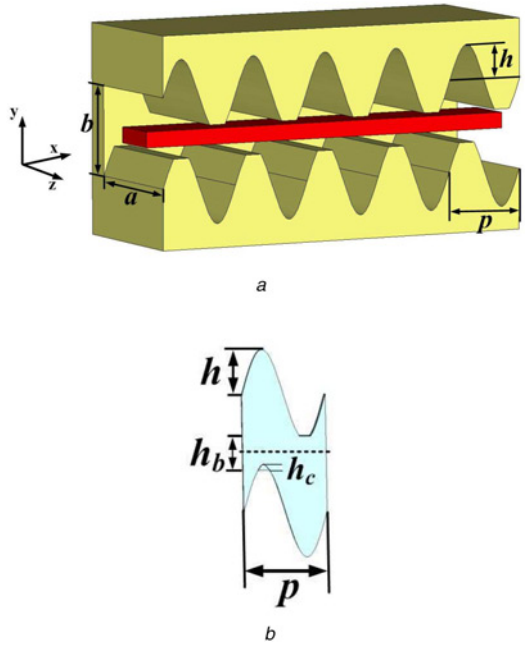

Fig. 1 *3D model and dimensional parameters of the TSWG SWS*
a Perspective view
b Single period structure

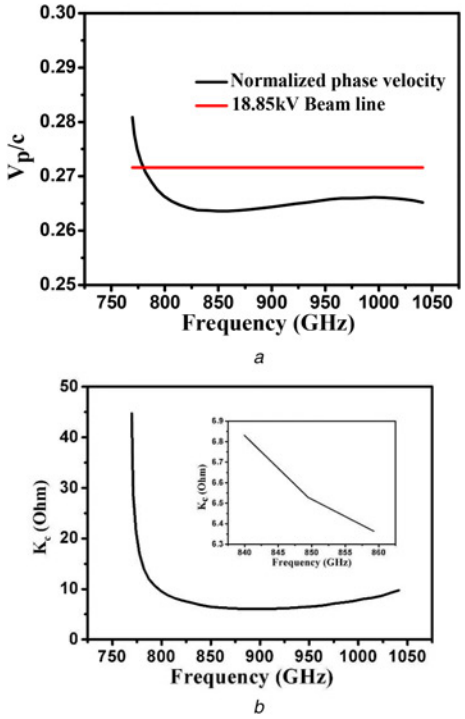

Fig. 2 *High-frequency characteristics of the 0.85 THz TSWG SWS*
a Dispersion curve and beam line
b Interaction impedance

of the device from the atmospheric environment and to transmit microwave power to the load. Therefore, the output window must satisfy some special requirements, such as low-energy reflection, relatively broad bandwidth, and high-power capability [21]. The pillbox window which is considered here consists of three parts, diamond window, cylinder waveguide and rectangular waveguide, respectively, shown in Fig. 4. As shown in Fig. 5, the pillbox

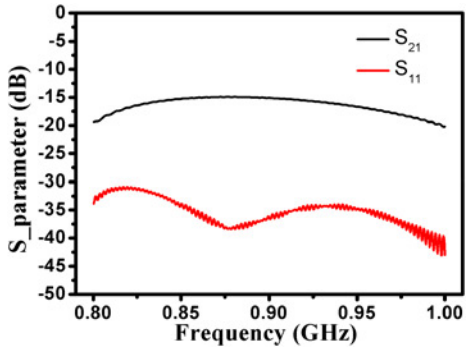

Fig. 3 *Transmission characteristics of 0.85 THz TSWG SWS*

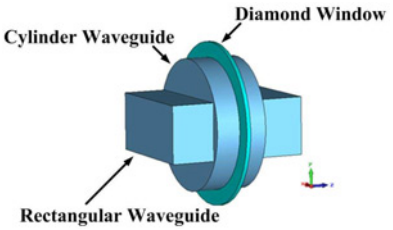

Fig. 4 *Pillbox window of 0.85 THz TSWG TWT*

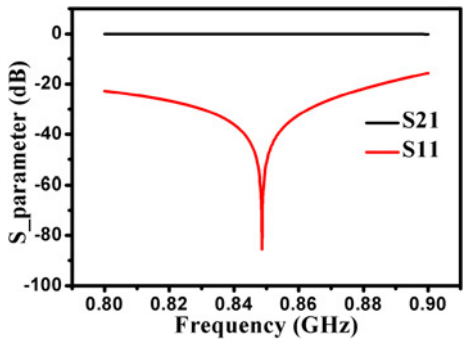

Fig. 5 *Transmission characteristics of 0.85 THz TSWG pillbox window*

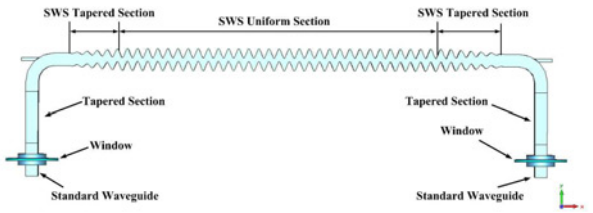

Fig. 6 *Overall structure of 0.85 THz TSWG TWT*

window transmission parameter S_{21} is more than −0.1 dB and the reflection parameter S_{11} is less than −20 dB from 0.8 to 0.885 THz.

Overall structures consist of several parts, such as high-frequency structure, tapered section, pillbox window and standard waveguide in Fig. 6. Due to the windows at both ends of the slow wave structure, transmission loss of the entire structure increases. As shown in Fig. 7, the reflection parameter S_{21} is less than −16 dB from 0.8 to 0.9 THz.

5 Beam–wave interaction characteristic

The simulation of beam–wave interaction process is completed by the 3D particle-in-cell algorithms. The dimension of sheet electron

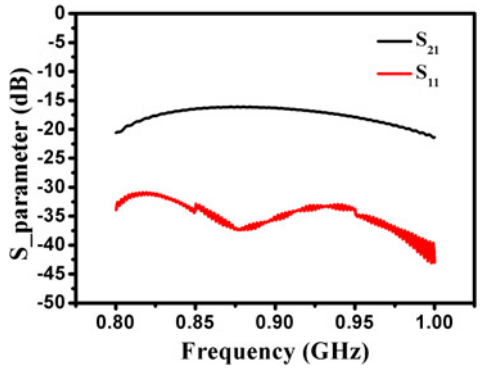

Fig. 7 *Transmission characteristics of overall structure of 0.85 THz TSWG TWT*

beam cross-sectional area is 97.5 × 18 μm^2, and the current of beam is set as 8 mA. The synchronous voltage of this beam–wave interaction model is 18.85 kV, and the power of input signal peak power is set as 3.025 mW. The amplitude of the focus magnetic field is set to 0.8 T to achieve 100% electron beam transport.

Fig. 8 shows the amplitudes of the input and output signals, which are monitored at the input and output port. From this figure, we observe that the output signal become stable after 1.25 ns and the input signal of 0.055 V is amplified to 0.73 V with the gain of 22.45 dB. From the Fourier transform of the output signal, the spectrum can be obtained, as illustrated in Fig. 9. The spectrum of the output signal is relatively pure at 0.85 THz.

Fig. 10 shows the electron energy as a function of the axial distance at 2.8 ns when the electron dynamic system is in a steady state. Most electrons in the spent beam have lost some kinetic energy, which has been transferred to the high-frequency electromagnetic fields. As a result, the driven signal is amplified. The inset demonstrates the electron bunching phenomenon at the end of the beam–wave interaction circuit.

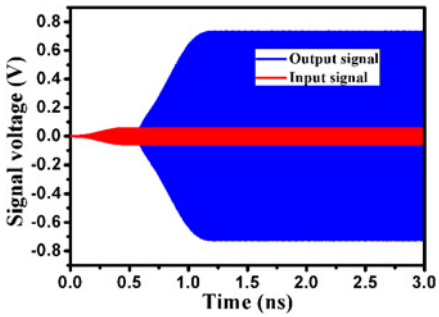

Fig. 8 *Input and output signals of the 0.85 THz TSWG TWT*

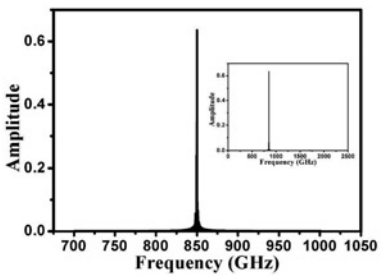

Fig. 9 *Spectrum of the output signal*

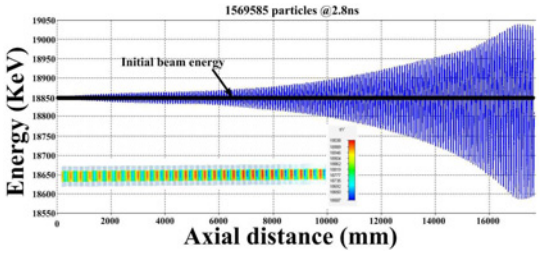

Fig. 10 *Electron energy as a function of the axial distance at 2.8 ns, and the inset gives the electron bunching at the end of the beam–wave interaction circuit*

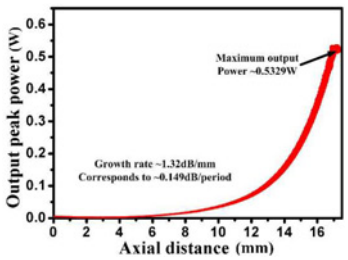

Fig. 11 *Output peak power as a function of the axial distance at 0.85 THz*

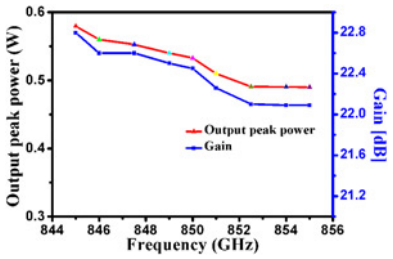

Fig. 12 *Output power and gain of the beam–wave interaction model*

Fig. 11 shows the output power as the function of the axial distance at the typical operating frequency of 0.85 THz. In this figure, we note that the amplified power saturates at 0.5329 W with a growth rate of 1.32 dB/mm, corresponding to 0.149 dB/ period.

Fig. 12 shows the output peak power and gain of the beam–wave interaction model in the operating frequency range of 0.844–0.855 THz. From the figure, the output peak power is >490 mW and the gain of the beam–wave interaction is >22.09 dB in the operating frequency range of 0.844–0.855 THz.

6 Conclusion

In summary, as a novel type of the SWS, TSWG SWS can be suggested as a promising beam–wave interaction circuit in the terahertz band because of its excellent transmission properties and large average interaction impedances. Its high-frequency characteristics, transmission characteristics of high-frequency system and beam–wave interaction characteristics are investigated by simulation method. In the terahertz band, metal loss must be considered carefully because it seriously affects the output power of the TWT. When we consider the metal loss under actual conditions, the output power of the whole tube is 490 mW from 0.844 to 0.855 THz. During the design process, we also designed a pillbox window for 0.85 THz TWT, which also meets our design requirements. Therefore, the TSWG TWT will be a very promising terahertz radiation source for lots of applications.

7 Acknowledgments

This work was supported in part by the National Natural Science Foundation of China (grant no. 61271029).

8 References

[1] Booske J H., Dobbs R.J., Joye C.D., *ET AL.*: 'Vacuum electronic high power terahertz sources', *IEEE Trans. Terahertz Sci. Technol.*, 2011, **1**, (1), pp. 54–75, doi: 10.1109/TTHZ.2011.2151610

[2] Tucek J.C., Basten M.A., Gallagher D.A., *ET AL.*: '0.850 THz vacuum electronic power amplifier'. Vacuum Electronics Conf., IEEE Int, 2014, pp. 1–2

[3] Berry D., Deng H., Dobbs R., *ET AL.* 'Practical aspects of EIK technology', *IEEE Trans. Electron Devices*, 2014, **61**, (6), pp. 1830–1835, doi: 10.1109/TED.2014.2302741

[4] Booske J.H.: 'Micromachined TWTs for THz radiation sources', 2001

[5] Bhattacharjee S., Booske J.H., Kory C.L., *ET AL.*: 'Folded waveguide traveling-wave tube sources for terahertz radiation', *IEEE Trans. Plasma Sci.*, 2004, **32**, (3), pp. 1002–1014, doi: 10.1109/TPS.2004.828886

[6] Shin Y.-M., Barnett L.R.: 'Intense wideband terahertz amplification using phase shifted periodic electron-plasmon coupling', *Appl. Phys. Lett.*, 2008, **92**, (9), pp. 091501-1–091501-3, doi: 10.1063/1.2883951

[7] Shin Y.-M., Barnett L.R., Luhmann N.C.: 'Strongly confined plasmonic wave propagation through an ultra wide band staggered double grating waveguide', *Appl. Phys. Lett.*, 2008, **93**, (22), pp. 221504-1–221504-3, doi: 10.1063/1.3041646

[8] Xu X., Wei Y.Y., Shen F., *ET AL.*: 'Sine waveguide for 0.22-THz traveling-wave tube', *IEEE Electron Dev. Lett.*, 2011, **32**, (8), pp. 1152–1154, doi: 10.1109/LED.2011.2158060

[9] Xu X., Wei Y.Y., Shen F., *ET AL.*: 'A watt-class 1-THz backward-wave oscillator based on sine waveguide', *Phys. Plasmas*, 2012, **19**, (1), pp. 013113-1–013113-4, doi: 10.1063/1.3677889

[10] Xu X., Wei Y., Shen F., *ET AL.*: 'A watt-class 1-THz backward-wave oscillator based on sine waveguide', *Phys. Plasmas*, 2012, **19**, (1), p. 132, doi: 10.1063/1.3677889

[11] Joye C.D., Cook A.M., Calame J.P., *ET AL.*: 'Demonstration of a high power, wideband 220-GHz traveling wave amplifier fabricated by UV-LIGA', *IEEE Trans. Electron Devices*, 2014, **61**, (6), pp. 1672–1678, doi: 10.1109/TED.2014.2300014

[12] Gong H., Travish G., Xu J., *ET AL.*: 'High-power tunable terahertz radiation by high-order harmonic generation', *IEEE Trans. Electron Devices*, 2013, **60**, (1), pp. 482–486, doi: 10.1109/TED.2012.2227751

[13] Mineo M., Paoloni C.: 'Double-corrugated rectangular waveguide slow-wave structure for terahertz vacuum devices', *IEEE Trans. Electron Devices*, 2010, **57**, (11), pp. 3169–3175, doi: 10.1109/TED.2010.2071876

[14] Mineo M., Paoloni C.: 'Improved corrugation cross-sectional shape in terahertz double corrugated waveguide', *IEEE Trans. Electron Devices*, 2012, **59**, (11), pp. 3116–3119, doi: 10.1109/TED.2012.2216534

[15] Zhang L., Wei Y., Guo G., *ET AL.*: 'A ridge-loaded sine waveguide for G-band traveling-wave tube', *IEEE Trans. Plasma Sci.*, 2016, **44**, (11), pp. 2832–2837, doi: 10.1109/TPS.2016.2605161

[16] Lei X., Wei Y., Wang Y., *ET AL.*: 'Full-wave analysis of the high frequency characteristics of the sine waveguide slow-wave structure', *AIP Adv.*, 2017, **7**, (8), p. 085111, doi: 10.1063/1.4997329

[17] Zhang L., , Wei Y., Jiang X., *ET AL.*: 'A truncated sine waveguide for G-band TWT'. IEEE Int. Vacuum Electronics Conf., London, United Kingdom, 2017

[18] Ansoft Corp.: Ansoft HFSS User's Reference. Available at: http://www.ansoft.com.cn/

[19] CST Corp.: CST MWS Tutorials. Available at: http://www.cstchina.cn/

[20] Kirley M.P., Booske J.H.: 'Terahertz conductivity of copper surfaces', *IEEE Trans. Terahertz Sci. Technol.*, 2015, **5**, (6), pp. 1012–1020, doi: 10.1109/TTHZ.2015.2468074

[21] Zhu F, Zhang Z.-C, Luo J.-R.: 'Investigation of the failure mechanism for an S-band pillbox output window applied in high-average-power klystrons', *IEEE Trans. Electron Devices*, 2010, **57**, (4), pp. 946–951, doi: 10.1109/TED.2010.2041874